ISSN 1024-8560, Atmospheric and Oceanic Optics, 2025, Vol. 38, No. 2, pp. 206–215. © Pleiades Publishing, Ltd., 2025.
Russian Text © The Author(s), 2024, published in Optika Atmosfery i Okeana.

OPTICAL MODELS AND DATABASES

Dynamics of Distribution of Aerosol Fractions in the Surface Air of the Boreal Zone of Western Siberia (Based on Observations at the Fonovaya Observatory)—Part 1: Comparison of the Periods of Summer Vegetation and Winter Dormancy of Woody Plants

M. P. Tentyukov[a, b, *], D. A. Timushev[c], D. V. Simonenkov[a], B. D. Belan[a], K. A. Shukurov[d], and A. V. Kozlov[a]

[a] *V.E. Zuev Institute of Atmospheric Optics, Siberian Branch, Russian Academy of Sciences, Tomsk, 634055 Russia*
[b] *Pitirim Sorokin Syktyvkar State University, Syktyvkar, 167001 Russia*
[c] *Institute of Physics and Mathematics of the Federal Research Center, Komi Research Center, Urals Branch, Russian Academy of Sciences, Syktyvkar, 167000 Russia*
[d] *Obukhov Institute of Atmospheric Physics, Russian Academy of Sciences, Moscow, 119017 Russia*
**e-mail: mpt@iao.ru*

Received May 7, 2024; revised September 13, 2024; accepted October 10, 2024

Abstract—We present the results of comparative characterization of fractional composition of surface aerosols in the period of summer vegetation and winter dormancy of woody plants in the boreal zone of Western Siberia. The article presents statistics on the size distribution of aerosol particles at the Fonovaya Observatory of IAO SB RAS (Tomsk Region) from July 1, 2022, to June 30, 2023. The analysis of the ratios of aerosol fractions revealed a paradoxical situation, where the number concentration of aerosol particles 0.3–2.0 μm diameter turned out to be significantly higher in winter than in summer. A phenomenological model is suggested which describes this effect as a manifestation of the action of radiometric forces.

Keywords: atmospheric aerosols, boreal forest, aerosol lifetime, coniferous, radiometric photophoresis, deciduous, forest canopy, aerosol stability

DOI: 10.1134/S102485602470177X

INTRODUCTION

The effect of the feedback mechanism in the "forest–aerosols–climate" system has been actively studied in the framework of the hypothesis, first formulated in work [1]. This hypothesis states that the global increase in air temperature and CO_2 concentration in the atmosphere entails the intensification of activity of photosynthesis and the growth of biomass of plants. It is noted that this should lead to the increased emission of non-methane biogenic volatile secondary organic aerosols in boreal forests [2]. However, photosynthetic enzymes are effective only in the warm season. At the same time, researchers overlook such an important additional source of secondary aerosols as the products of metabolic reactions synthesized by certain plants in the winter period [3]. These are coniferous plants, occupying about 80% of the area of boreal forests in Russia [4], as well as epiphyte lichens.

It is now becoming clear that lichens can influence the chemical composition of the atmosphere. For instance, volatile organic compounds (exometabolites) released by lichens to the environment exhibit high chemical activity [5]. After entering the environment, they favor the generation of secondary aerosols and their growth [5, 6]. In this regard, we note that the effect of exometabolites of coniferous plants and epiphyte lichens on the size distribution of surface aerosols during the winter dormancy period of plants is as yet poorly studied.

The purpose of this work is to study the specific features of the dynamics of the distribution of number concentration of surface aerosols in different vegetation phases of deciduous and coniferous trees.

MATERIALS AND METHODS

Method of Measuring Aerosol Number Concentration

The continuous measurements of aerosol particle size distribution were carried out using a Grimm 1.108 aerosol spectrometer [7] installed at the Fonovaya Observatory (Institute of Atmospheric Optics, Siberian Branch, Russian Academy of Sciences, Tomsk (IAO)). The number concentration (N, dm^{-3}) of aerosols in the diameter (d) range from 0.3 to 20 μm

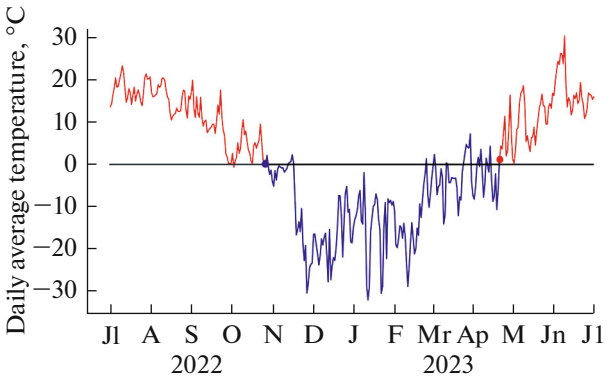

Fig. 1. Time interval for the warm (red curve) period of photosynthesis, with a mark of its beginning on April 20, 2023, and for the cold period (blue curve), with a mark of its beginning on October 26, 2022; from here on, J stands for January, F for February, Mr for March, Ap for April, M for May, Jn for June, Jl for July, A for August, S for September, O for October, N for November, and D for December.

divided in 15 subranges was hourly measured for 10 min with preliminary 3-min isokinetic pumping from an airflow in a wind tunnel from the altitude of 4.9 m.

Statistical Estimate of Time Dynamics of Size Spectrum of Surface Aerosol

The statistical parameters of the size distribution of surface aerosols were calculated from a sample compiled using a continuous measurement time series within the time interval from July 1, 2022, to June 30, 2023. This sample encompasses the entire phase of the winter plant dormancy during winter 2022/23; the sample size was 8760 hourly observations. Servicing software was written to work with the sample and to estimate how the size spectra of surface aerosols are related to meteorological data.

Substantiation of the Choice of Temperature Limits for Photosynthesis

At temperatures from 0 to +10°C, the enzymes responsible for photosynthesis are inefficient, and this reduces the photosynthesis rate. At the same time, the temperature limits within which photosynthesis can occur differ for plants in different climatic zones. For instance, the minimal temperature for plant photosynthesis in the temperate and middle latitude belt is ~0°C; while for tropical plants it is +5 to +10°C. Therefore, in this paper, the time limits of the warm and cold periods in the plant life cycle are referenced to the dates with a certain temperature mark. The start (end) of the warm period of photosynthesis for the study area was counted off from the date when the daily average temperature was established to be above (below) 0°C. The start of the cold period was set to the date of establishing the daily average temperatures below 0°C; and the cold period ended when the daily average temperature was stably above 0°C (Fig. 1).

Statistical Processing

In this paper, samples were handled using the median, which is convenient in that it is not very sensitive to the occurrence of individual extreme values in the sample. The median is an asymptotically normal random quantity described by the Weibull distribution function [8]. This function better characterizes the data for which the presence of normal, logarithmically normal, or any other distribution law is difficult to anticipate. The median can be applied even if a set under study comprises a certain number (up to 25%) of "zero" samples.

The median is more stable than the arithmetic mean under the conditions of excessive (sharp-topped) distributions and, more importantly, it does not depend on the distribution law of a random quantity, because its position does not change upon any calculation transforms of the parameter under study. This latter is very important in our situation, when a single type of particle distribution can hardly be anticipated beforehand for each aerosol size fraction. The seasonal dynamics of the size distribution of surface aerosols were visualized using columnar and linear diagrams. The former were plotted using median values, and the latter were plotted using the sliding average. This latter made it possible to smooth out sharp peaks and to identify the common tendencies in seasonal dynamics of the size distribution of aerosol particles.

Trajectory Analysis of Air Mass Transport

The trajectory analysis over the observation site was carried out using 7-day back trajectories calculated by refined method [9] using the trajectory model NOAAHYSPLIT_4 [10] and based on the grid archive of meteorological data NCEP GFS1p0 with a resolution of 1° in longitude and latitude. The calculations took into account only those fragments of air mass transport trajectories, which fell within the regional atmospheric boundary layer (ABL) until their arrival at the lower troposphere over the Fonovaya Observatory. In other words, if a trajectory fragment in any region was above the ABL, it was not used in the transport probability calculation. The calculations were performed for all levels above the surface from 100 to 2100 m with a step of 100 m for the lower troposphere. Back trajectories started in backward model time (ended in real time) at all indicated levels every hour (00:00 UTC, 01:00 UTC, etc.) in the period from July 1, 2022, to June 30, 2023. The thus obtained back trajectory set was used, applying method [11], to calculate the fields of the monthly average probability of air particle transport in the regional-scale ABL, which allows

us to judge the potential aerosol sources for the lower troposphere over the Fonovaya Observatory.

RESULTS AND DISCUSSION

Comparative Analysis of Relationship between Surface Aerosols Fractions in Warm and Cold Periods of Photosynthesis

The results of statistical processing of the sample are presented in Table 1. Note the strong dispersion of the coefficients of variation for aerosol particles with d from 0.3 to 3.0 μm. The coefficients of variations vary from 118 to 214% (93–124%) for the warm (cold) period. Such values for the cold period are due to the absence of emissions of biogenic volatile secondary organic aerosols associated with deciduous trees. At the same time, the relatively sharp increase in the coefficient of variations for aerosol particles with $d >$ 3.0 μm is associated with the winter effect of local sources [12].

If we compare the average number concentrations of surface aerosols (Fig. 2), we can note that they are paradoxically lower in the warm period than in the winter period of photosynthesis, despite the fact that the total area of leaf surface is incomparably larger in summer than in winter forest canopy. This is because the lifetime of summer aerosols is shorter than the lifetime of winter aerosols.

Aerosols can deposit onto the Earth's surface due to turbulent and gravitational sedimentation, as well as due to washout by precipitation (moist deposition). However, if we consider the aerosol particle deposition rate as a function of the particle diameter, the sedimentation mechanism for small particles (with d from 0.01 to 10.0 μm) is predominantly determined by turbulent diffusion [13]. On the contrary, the gravitational sedimentation becomes more important if the particle diameter >10.0 μm. However, the wintertime increase in the number concentration of particles with d = 0.3–0.4 to 1.6–2.0 μm gives grounds to believe that the manifestation of these two mechanisms in winter is complicated by the effect of radiometric photophoresis.

Snow cover under any conditions, and even at the lowest temperature, emits intrinsic heat in the form of longwave radiation and shows a high ability to reflect solar radiation. In the field of infrared radiation leaving the snow cover, positive, so-called snow, photophoresis [3] and the associated subvertical motions of aerosols counteracting the gravity force (photophoretic levitation [14]) can occur. Evidently, snow photophoresis can be a significant seasonal factor of vertical aerosol transport in the field of infrared radiation formed over the snow cover. Therefore, the observed paradoxical effect of the wintertime increase in the number concentration of fine aerosols stems from snow photophoresis, when turbulent sedimentation of fine aerosol in the surface air layer is already ineffective, while the gravitational sedimentation is still ineffective. This gives rise to diffusion-gravitational equilibrium, where particles hang above (levitate) over the snow cover in the field of infrared radiation emitting by the snow cover. This increases the aerosol lifetime in the winter forest canopy and leads to an increase in the number concentration of aerosol particles of certain sizes, being the fractions with d = 0.3–0.4 to 1.6–2.0 μm in our case.

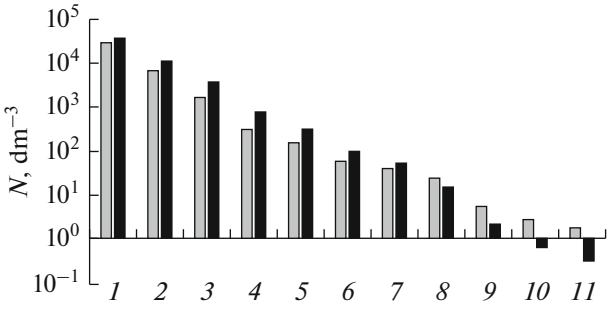

Fig. 2. Relationship of the number concentrations of surface aerosol in the warm (gray columns) and cold (black columns) period of photosynthesis among different fractions of surface aerosol: d = 0.3–0.4 (columns *1*); 0.4–0.5 (columns *2*); 0.5–0.65 (columns *3*); 0.65–0.8 (columns *4*); 0.8–1.0 (columns *5*); 1.0–1.6 (columns *6*); 1.6–2.0 (columns *7*); 2.0–3.0 (columns *8*); 3.0–4.0 (columns *9*); 4.0–5.0 (columns *10*); and 5.0–7.5 μm (columns *11*).

Features of Dynamics of Fractional Composition of Surface Aerosols in Summer Vegetation and Winter Dormancy of Woody Plants

The daily and seasonal dynamics of the size spectrum of surface aerosols were estimated using continuous measurement series from July 1, 2022, to June 30, 2023. The continuous measurements of aerosol distribution in specific periods of time were represented graphically using servicing software to visualize the specific features of the dynamics of distribution of aerosol fractions in different vegetation phases of deciduous and coniferous plants (Fig. 3). In order for all dynamics of aerosol size fractions to be displayed simultaneously in a single row in a chosen time interval, the range of the ordinate axis in the monthly diagrams was determined from maximal and minimal median values of aerosol number concentration recorded for each size range.

Figure 3 shows predominance of particles with d = 0.3–4.0 μm in December, January, and February in the surface atmosphere. After sap flow and bud swelling begin in deciduous plants, the concentration of small particles with d = 0.3–0.65 μm is barely detectable. However, after the leaves are out and until trees are completely covered with leaves (May to June), almost the entire range of particles is detected in the surface atmosphere. Then, in midsummer (July) in the

Table 1. Statistical parameters of the size composition of surface aerosol in warm and cold periods of photosynthesis

Parameter	d, μm														
	0.3–0.4	0.4–0.5	0.5–0.65	0.65–0.8	0.8–1.0	1.0–1.6	1.6–2.0	2.0–3.0	3.0–4.0	4.0–5.0	5.0–7.5	7.5–10.0	10.0–15.0	15.0–20.0	>20.0
Warm period of photosynthesis (July 1–October 25, 2022 + April 20–June 30, 2023)															
n_0	4467	4467	4467	4467	4467	4467	4457	4467	4467	4467	4467	4467	4467	4467	4467
$\bar{x}$	30488	7074	1620	326	158	60	43	25	6	3	1	0	0	0	0
δ	49352.5	11966.2	3177.5	698.7	304.5	96.1	50.8	30.9	9.6	5.1	2.8	0.6	0.2	0.1	0.0
min	365	65	17	7	3	0	0	0	0	0	0	0	0	0	0
Q_1	7114	1410.5	321.5	72	40	19	19	9	1	0	0	0	0	0	0
Me	14841	3219	708	143	73	31	30	16	3	1	1	0	0	0	0
Q_3	30487.5	6881	1618.5	326	160	64	51	31	7	3	1	0	0	0	0
max	640730	227244	107333	27885	10036	2790	1066	622	185	67	31	11	4	1	2
v	162	169	196	214	193	161	118	124	162	173	189	–	–	–	–
n_1	2296	2269	2211	27885	2122	2071	2065	1963	1472	1157	849	269	78	14	1
n_2	51.4	50.7	49.5	624.2	47.5	46.3	46.3	43.9	32.9	25.9	19.0	6.0	1.7	0.3	0.02
Cold period of photosynthesis (October 26, 2022–April 19, 2023)															
n_0	4218	4218	4218	4218	4218	4218	4218	4218	4218	4218	4218	4218	4218	4218	4218
$\bar{x}$	33011	10369	3341	726	311	91	45	16	2	1	0	0.06	0.03	0.01	0
δ	37500.0	12733.4	4141.6	837.4	319.3	84.8	42.4	17.8	3.6	1.4	0.9	0.29	0.2	0.09	0.04
min	303	63	27	9	5	1	1	0	0	0	0	0	0	0	0
Q_1	10307.75	2711.25	925	237	114	34	18	4	0	0	0	0	0	0	0
Me	21401.5	6058.5	1956	456.5	209.5	65	33	10	1	0	0	0	0	0	0
Q_3	43092.25	13506.75	4423	961	408	124	62	21	3	1	1	0	0	0	0
max	467922	157395	58617	11551	3994	714	375	225	41	15	11	4	3	2	1
v	114	123	124	115	103	93	94	114	154	161	221	–	–	–	–
n_1	2057	2031	2054	2035	2018	1965	1937	1707	972	707	467	136	76	29	8
n_2	48.7	48.1	48.7	48.2	47.8	46.5	45.9	40.4	23.0	16.7	11.0	3.2	1.8	0.6	0.1

n_0 is the sample size; $\bar{x}$ is the arithmetical mean number concentration, dm^{-3}; δ is the standard deviation, dm^{-3}; min is the minimal value, dm^{-3}; Q_1 is the first quartile, dm^{-3}; *Me* is the median, dm^{-3}; Q_3 is the third quartile, dm^{-3}; max is the maximal value, dm^{-3}; v is the coefficient of variation, %; n_1 is the number of nonzero observations; and n_2 is the percentage of nonzero observations, %.

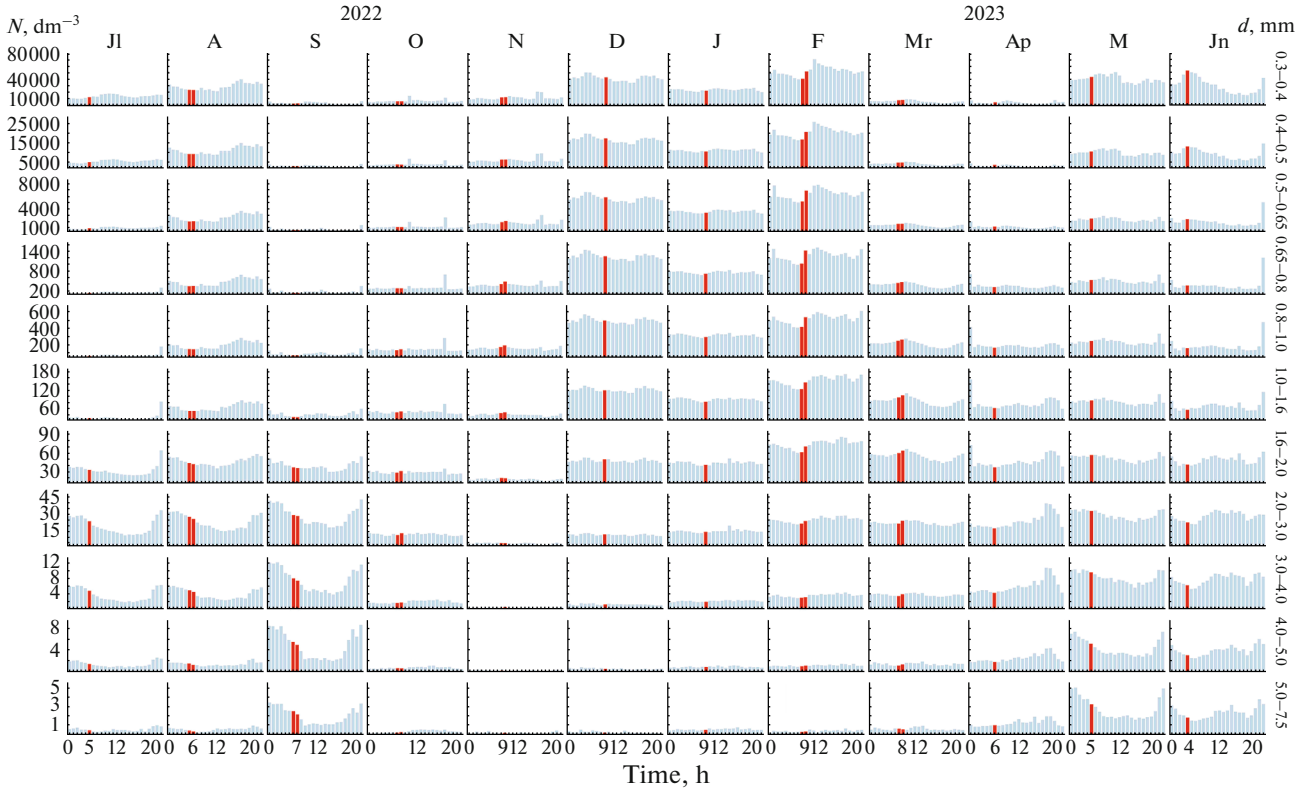

Fig. 3. Daily dynamics of the number concentrations of fractions of surface aerosol (morning measurements are highlighted by red).

blooming and ovary phase, "disappearance" of fine (d = 0.3–1.6 μm) and coarse ($d \geq$ 4.0–7.5 μm) fractions and dominance of the medium-size (d = 1.6–4.0 μm) fraction is recorded. The relationship among fractions again changes with the advent of the fruiting phase (August): fine and medium-size fractions are stably recorded in the surface atmosphere, with the coarse fraction becoming almost indiscernible.

Particles from 1.6 to 7.5 μm diameter are clearly predominant in the leaf blossoming and leaf fall phase (September). The period of transition to winter dormancy lasts for two months (October and November). The minimal number concentration of surface aerosols in all size intervals is recorded in this time. Then, the winter growth in emissions from coniferous trees and epiphyte lichens is observed, which are strongly obscured in the warm period of photosynthesis not so much due to the emissions from deciduous trees, but due to the growth of aerosol particles as a result of summertime turbulence activation in the forest canopy.

Thus, the graphical technique used for visualizing the results of statistical analysis of time evolution of aerosol number distribution coupled with phenological phases makes it possible to estimate in a new way a likely contribution of woody plants to the regional-scale aerosol climate.

Correlation between Meteorological Parameters and Number Concentration of Size Fractions of Surface Aerosols

The correlation analysis was carried out to identify the character of the interrelation between meteorological parameters and the number concentration of size fractions of surface aerosols. Based on it, we singled out two groups of particles (d = 0.3–2.0 and 2–7.5 μm). There is a week negative correlation with the temperatures in group 1, and a positive correlation in group 2 (Table 2).

However, these correlations should not be understood as a decrease in the concentration of fine aerosol fractions and a growth of the content of large particles with decreasing temperature. The correlation coefficient in group 1 becomes negative only when data for late December and November are taken into consideration (if these months are disregarded, the correlation coefficient is positive, as in group 2). Possibly, the volume of emissions in group 1 increases in this period for other reasons; however, the temperature in late November–December decreases, resulting in the negative correlation. If this is accepted, the presence of the negative correlation between the temperature and the growth in the number concentration of large particles indicates indirectly that the aerosol lifetime increases in the period of winter plant dormancy. As a result, the

Table 2. Correlations between meteorological parameters and the number concentrations of aerosols from different size fractions

Meteorological parameter	d, μm										
	group 1							group 2			
	0.3–0.4	0.4–0.5	0.5–0.65	0.65–0.8	0.8–1.0	1.0–1.6	1.6–2.0	2.0–3.0	3.0–4.0	4.0–5.0	5.0–7.5
T	−0.13	−0.20	−0.35	−0.42	−0.41	−0.27	0.12	0.51	0.49	0.34	0.31
T_{min}	−0.15	−0.21	−0.35	−0.43	−0.42	−0.29	0.07	0.45	0.42	0.28	0.25
T_{max}	−0.10	−0.17	−0.31	−0.39	−0.37	−0.23	0.17	0.56	0.53	0.38	0.36
P_0	0.12	0.16	0.27	0.32	0.30	0.19	−0.06	−0.31	−0.28	−0.10	−0.12
P	0.12	0.17	0.28	0.33	0.31	0.19	−0.07	−0.33	−0.29	−0.12	−0.13
U	0.05	0.06	0.05	0.03	0	−0.06	−0.21	−0.35	−0.37	−0.32	−0.36
VV	0.01	−0.01	−0.05	−0.08	−0.09	−0.05	0.11	0.29	0.30	0.26	0.23
T_d	−0.13	−0.19	−0.34	−0.42	−0.41	−0.28	0.09	0.46	0.43	0.28	0.25
RRR	−0.06	−0.06	−0.08	−0.09	−0.08	−0.06	−0.02	0.01	−0.03	−0.08	−0.09
sss	0.27	0.33	0.45	0.52	0.51	0.43	0.15	−0.24	−0.29	−0.23	−0.22

Meteorological data are imported from https://rp5.ru/Weather_in_Kozhevnikovo,_Tomsk_olast. Here, T is the temperature; P_0 is the atmospheric pressure at station altitude; P is the atmospheric pressure reduced to the mean sea level; U is the relative humidity; VV is the horizontal visibility range; T_d is the dew-point temperature; RRR is the precipitation amount; and sss is the height of snow cover.

number of large aerosols increase in each particle size range. This is very similar to the domino effect, when the particle growth (coagulation) wave passes from one size range to the neighboring one.

Aerosol Effects during Long-Range and Regional Transports: Anomalous Character of Aerosol Field

Correlation coefficients (Table 3) were calculated to estimate the relationships between the concentrations of aerosol fractions. One can note that the size fractions are divided into two blocks with respect to cross-correlations. The first block comprises the particles with d = 0.3–0.4; 0.4–0.5; 0.5–0.65; 0.65–0.8; 0.8–1.0; 1.0–1.6, and 1.6–2.0 μm, and in the second block includes particles with d = 2.0–3.0; 3.0–4.0; 4.0–5.0, and 5.0–7.5 μm. It is noteworthy that there is a high positive cross-correlation inside these blocks (bolded in Table 3).

An examination for the presence of interrelation between the number concentrations of aerosols of different sizes and meteorological parameters using a multiple regression model (the dependence of the concentration of each fraction on all weather variables at once) gave no results: the coefficients of determination were low. The inclusion in the calculations of weather parameters with a lag revealed no significant correlations as well. However, we revealed one strange circumstance: many quite significant bursts in the number concentration of surface aerosols in the final data. In Fig. 4, these bursts are shown as peaks with marks above the line represented by a sliding average. These peaks are not associated with the weather conditions; however, they make quite a significant contribution to the statistics. These peaks show no time periodicity. However, if this circumstance is considered in combination with the dynamics of the distribution of aerosol fractions in different phenological phases, the number concentration of large aerosols increases due to aggregation of small particles, the concentration of which increases due to their excessive generation during photosynthesis in the warm period.

On the contrary, deciduous trees do not participate in the generation of secondary organic aerosols in winter; therefore, the contribution of biogenic volatile secondary organic aerosols in the wintertime aerosol field over the Fonovaya Observatory is totally controlled by coniferous trees and epiphyte lichens. Against this background, the winter and autumn bursts of excessive concentration of aerosols may be both due to local sources [12], and to long-range transport.

The probability of the air mass transport from droughty belt in the south of Russia within the boundaries 40°–50° N, 50°–80° E (Kazakhstan and north of the Aral–Caspian arid region) is much larger in the cold (October–March) than the warm (April–September) season (Fig. 5) [9, 15]. Hence, the effect of mineral aerosols cannot be totally excluded, though according to satellite (Aqua-AMSR) measurements, in 2022–2023 in this droughty region, soil was much wetter in the cold season than in the warm (Fig. 6).

It should be noted that the high occurrence frequency of long-range transitions from the Aral–Caspian region gives grounds to consider it as the main off-season source of fine aerosol fraction, because,

Table 3. Correlation between the number concentrations in different aerosol size fractions

d, μm	0.3–0.4	0.4–0.5	0.5–0.65	0.65–0.8	0.8–1.0	1.0–1.6	1.6–2.0	2.0–3.0	3.0–4.0	4.0–5.0	5.0–7.5
0.3–0.4	**1**										
0.4–0.5	**0.99**	**1**									
0.5–0.65	**0.94**	**0.97**	**1**								
0.65–0.8	**0.89**	**0.92**	**0.98**	**1**							
0.8–1.0	**0.87**	**0.90**	**0.96**	**0.99**	**1**						
1.0–1.6	**0.85**	**0.86**	**0.91**	**0.94**	**0.97**	**1**					
1.6–2.0	**0.73**	**0.71**	**0.70**	**0.71**	**0.76**	**0.88**	**1**				
2.0–3.0	0.29	0.24	0.18	0.16	0.21	0.40	**0.76**	**1**			
3.0–4.0	0.09	0.04	−0.01	−0.02	0.03	0.20	0.58	**0.94**	**1**		
4.0–5.0	−0.02	−0.05	−0.07	−0.06	−0.03	0.08	0.38	**0.72**	**0.86**	**1**	
5.0–7.5	−0.01	−0.04	−0.06	−0.05	−0.02	0.11	0.41	**0.76**	**0.90**	**0.97**	**1**

under arid conditions, aerosol is constantly generated by the underlying surface and dispersed by convective and vortical flows in the ABL and consequently to the troposphere with a high probability [16, 17]. This off-season effect of the Aral–Caspian region obscures the oscillations in particle size composition in the aerosol field over the Fonovaya Observatory in the periods of both summertime vegetation (to a lesser degree) and wintertime dormancy of woody plants (to a higher degree). However, the effect of the woody plants on the relationship between percentages of mineral and organic aerosols can be estimated more accurately after analysis of the chemical composition of aerosol samples from different fractions.

The spring–summer anomalous increases in the number concentration of aerosol fractions 0.3–0.4 to 1.6–2.0 μm (see Fig. 3) deserve a special explanation. The turbulence development in the surface air layer is determined by the gradient and daily behavior of the temperature in the active layer. On the other hand, in forest the role of the active surface is played by crowns. During fair weather, crown surface is strongly heated due to the influx of solar radiation. At the same time, the forest plants are heated differently at different height levels due to the nonuniform distribution of solar radiation and temperatures in forest canopy [18]. Therefore, this temperature distribution creates favorable conditions for the development of convection and turbulence in tree crowns. This should lead to faster turbulent sedimentation of aerosols and a lower aerosol number concentration in the surface air layer. However, the cases considered above exhibit a reverse

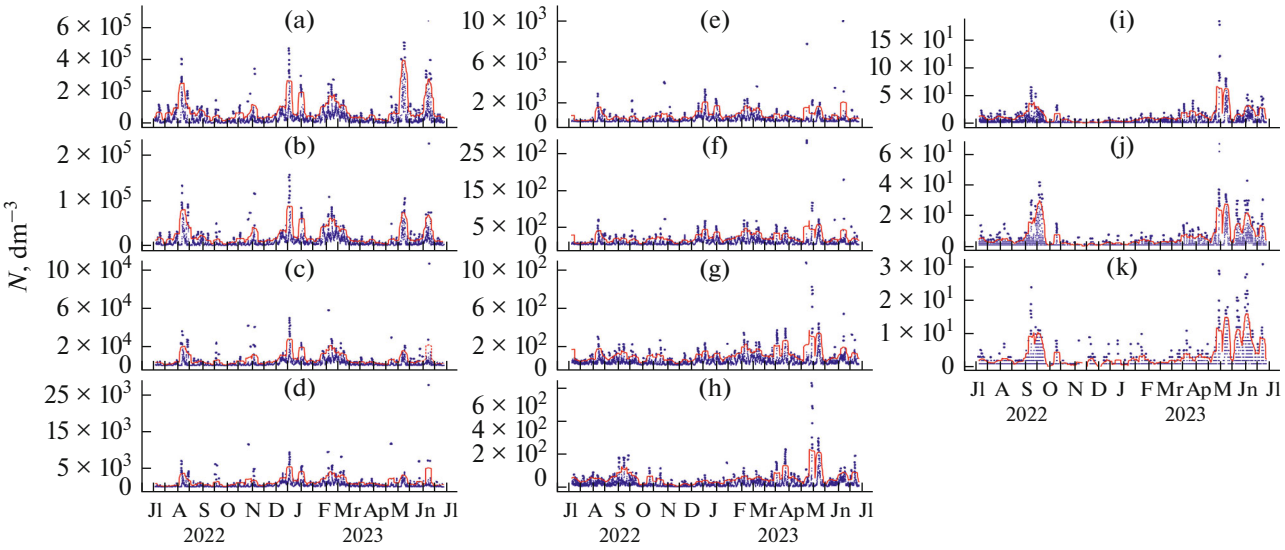

Fig. 4. Seasonal anomalous bursts with outliers above red line, represented by sliding average, of the number concentration of individual fractions of atmospheric aerosol: (a) d = 0.3–0.4; (b) 0.4–0.5; (c) 0.5–0.65; (d) 0.65–0.8; (e) 0.8–1.0; (f) 1.0–1.6; (g) 1.6–2.0; (h) 2.0–3.0; (i) 3.0–4.0; (j) 4.0–5.0; and (k) 5.0–7.5 μm.

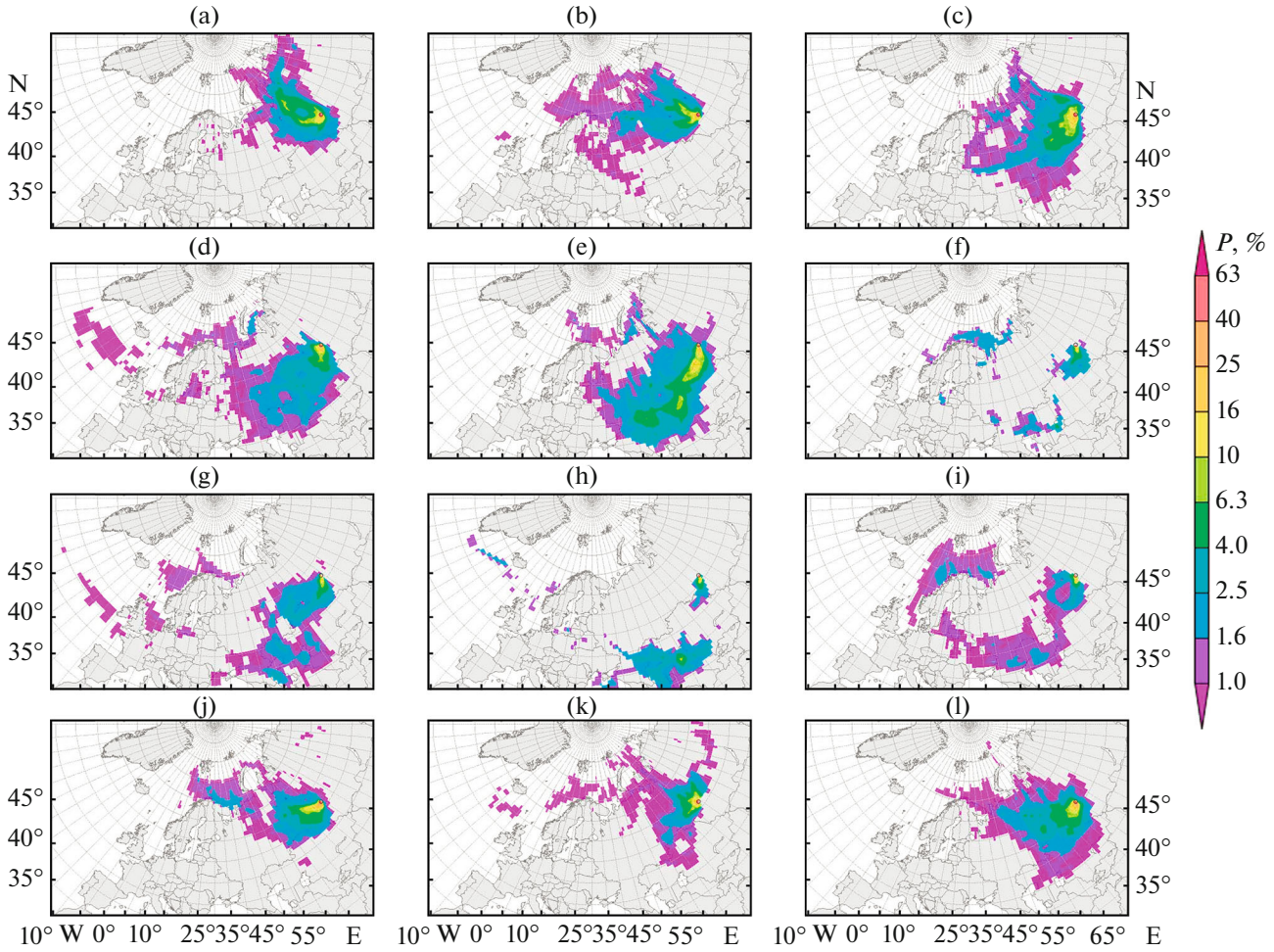

Fig. 5. Monthly average regional probability of air mass transport within the ABL in the lower troposphere (100–2100 m) over the Fonovaya Observatory: (a) June 2022, (b) August 2022, (c) September 2022, (d) October 2022, (e) November 2022, (f) December 2022, (g) January 2023, (h) February 2023, (i) March 2023, (j) April 2023, (k) May 2023, (l) June 2023.

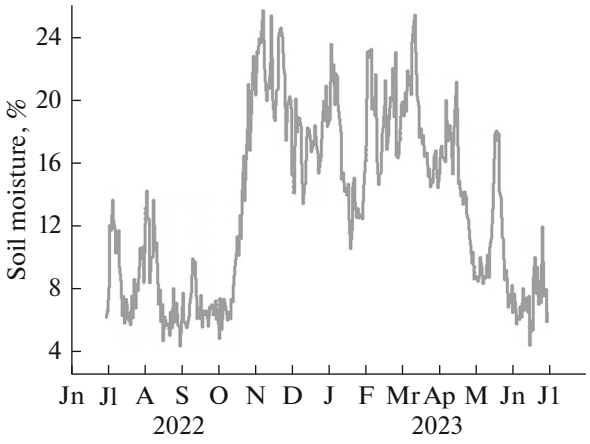

Fig. 6. Variations in daily soil moisture in the period from July 1, 2022, to June 30, 2023, within the boundaries 40°–50° N, 50°–80° E (droughty belt to the south of Russia) using Aqua-AMSR data.

pattern. Presumably, this is due to the action of forces of a radiometric nature, prohibiting the turbulent sedimentation of aerosol and initiating subvertical motions of aerosols against the gravity force (photometric levitation [14, 19, 20]). It is noteworthy that the presence of temperature and radiation stratification in the canopy of the summertime forest can serve a kind of a trigger of the processes of radiometric photophoresis, possibly manifested in summertime anomalous bursts of aerosol number concentration. On the other hand, the increase in the number concentration of fine aerosol during winter can be due to the action of radiometric forces, initiated by the physical properties of the snow cover. They arise when the turbulent sedimentation of aerosols is no longer effective, while the gravitational sedimentation is still ineffective. In other words, there appears the diffusion-gravitational equilibrium, under which the particles hang (levitate) over this snow cover in the field of infrared radiation leav-

ing the snow cover. This increases the lifetime of fine aerosol fractions (i.e., particles with $d = 0.3–2.0$ μm in our case) and, hence, the particle number concentration in the surface air layer.

CONCLUSIONS

The comparison of continuous measurements of the number concentration of surface aerosol during the summer vegetation (warm period of photosynthesis) and winter dormancy (cold period of photosynthesis) of woody plants in a wide particle size range at the Fonovaya Observatory of Institute of Atmospheric Optics, Siberian Branch, Russian Academy of Sciences (Tomsk oblast) in the period from July 1, 2022, to June 30, 2023, revealed a paradoxical situation, when the number concentration of aerosol particles 0.3–2.0 μm diameters turned out to be higher in winter than in summer. It is proved that this phenomenon is caused by the action of radiometric forces and, in particular, by snow photophoresis. These forces can compete with the gravity forces, thereby ensuring the conditions for the particle levitation over snow surface in the surface air layer, increasing the life time and the number concentration of particles with $d = 0.3–2.0$ μm. Evidently, this affects the radiation balance of the winter atmosphere; therefore, the vertical particle motions under the action of photophoretic forces should be taken into consideration when constructing transport models of vertical aerosol transport in the lower troposphere. Moreover, radiometric photophoresis, in addition to the long-range transport of admixtures with moisture-carrying air masses, can be justifiably considered as one of the potentially significant mechanisms of the vertical aerosol transport in the surface atmosphere when the wintertime aerosol field is formed.

FUNDING

This work was supported by the Ministry of Science and Higher Education of the Russian Federation (V.E. Zuev Institute of Atmospheric Optics, Siberian Branch, Russian Academy of Sciences). The trajectory analysis supported by the Russian Center for Scientific Information (RCNI) and Iran National Science Foundation (INSF) (project no. 20-55-56028).

CONFLICT OF INTEREST

The authors of this work declare that they have no conflicts of interest.

REFERENCES

1. M. Kulmala, T. Suni, K. E. J. Lehtinen, MasoM. Dal, M. Boy, A. Reissell, U. Rannik, P. Aalto, P. Keronen, H. Hakola, J. Back, T. Hoffmann, T. Vesala, and P. Hari, "A new feedback mechanism linking forests, aerosols, and climate," Atmos. Chem. Phys. **4** (2), 557 (2004).
2. M. Kulmala, I. Riipinen, and V.-M. Kerminen, "Aerosols and climate change," in *From the Earth's Core to Outer Space*, Ed. by I. Haapala (Springer, Berlin, Heidelberg, 2012).
3. M. P. Tentyukov, B. D. Belan, D. V. Simonenkov, and V. I. Mikhailov, "Generation of secondary organic aerosols on needle surfaces and their entry into the winter forest canopy under radiometric photophoresis," Atmos. Ocean. Opt. **35** (5), 490–496 (2022).
4. http://www.priroda.ru/regions/forest/. Cited February 8, 2024.
5. M. Glasius and A. H. Goldstein, "Recent discoveries and future challenges in atmospheric organic chemistry," Environ. Sci. Technol. **50**, 2754–2764 (2016). https://doi.org/10.1021/acs.est.5b05105
6. J. Penuelas and M. Staudt, "BVOCs and global change," Trends Plant. Sci. **15**, 133–144 (2010). https://doi.org/10.1016/j.tplants.2009.12.005
7. J.-Ch. Soo, K. Monaghan, T. Lee, M. Kashon, and M. Harper, "Air sampling filtration media: Collection efficiency for respirable size-selective sampling," Aerosol Sci. Technol. **50** (1), 76–87 (2016). https://doi.org/10.1080/02786826.2015.1128525
8. B. A. Yufa and Yu. M. Gurvich, "Use of median and quartiles to assess normal and abnormal values of a geochemical field," Geokhimiya, No. **8**, 817–824 (1964).
9. K. A. Shukurov, D. V. Simonenkov, A. V. Nevzorov, A. Rashki, N. H. Hamzeh, S. F. Abdullaev, L. M. Shukurova, and O. C. Chkhetiani, "CALIOP-based evaluation of dust emissions and long-range transport of the dust from the Aral-Caspian arid region by 3D-Source Potential Impact (3D-SPI) Method," Remote Sens. **15** (5), 2819 (2023). https://doi.org/10.3390/rs15112819
10. R. R. Draxler and G. D. Hess, "An overview of the HYSPLIT_4 modeling system of trajectories, dispersion, and deposition," Aust. Meteorol. Mag. **47**, 295–308 (1998).
11. K. A. Shukurov and O. G. Chkhetiani, "Probability of transport of air parcels from the doi lands in the Southern Russia to Moscow region," Proc. SPIE **10466**, 104663V (2017). https://doi.org/10.1117/12.2287932arid
12. N. S. Evseeva, Z. N. Kvasnikova, M. A. Kashiro, and A. S. Batmanova, "Modern aeolian morpholithogenesis of cold period in the south-east part of the sub-taiga zone of the West Siberian Plain," Geosfernye Issled., No. 2, 6–13 (2017).
13. L. Khorvat, *Acid Rain,* Ed. by Yu.N. Mikhailovskii (Stroiizdat, Moscow, 1990) [in Russian].
14. S. A. Beresnev, F. D. Kovalev, L. B. Kochneva, V. A, Runkov, P. E. Suetin, and A. A. Cheremisin, "On the possibility of particle's photophoretic levitation in the stratosphere," Atmos. Ocean. Opt. **16** (1), 44–48 (2003).
15. *Soviet-American Experimental Study of Arid Aerosol,* Ed. by G.S. Golitsyn (NPO "Taifun", St. Petersburg, 1992) [in Russian].
16. G. V. Simonova, D. A. Kalashnikova, A. N. Markelova, A. S. Bondarenko, and A. E. Davydkina, "Variations in

the oxygen and hydrogen isotope composition of precipitation in Tomsk (2016–2020)," Opt. Atmos. Okeana **36** (7), 595–601 (2023). https://doi.org/10.15372/AOO20230709

17. E. B. Gledzer, I. G. Granberg, and O. G. Chkhetiani, "Air dynamics near the soil surface and convective emission of aerosol," Izv., Atmos. Ocean. Phys. **46** (1), 29–40 (2010).
18. V. A. Alekseev, *Light Regime of Forest* (Nauka, Leningrad, 1975) [in Russian].
19. L. B. Kochneva, Thesis of Candidate's Dissertation in Mathematics and Physics (Ekaterinburg, 2007).
20. V. Chernyak and S. Beresnev, "Photophoresis of aerosol particles," J. Aerosol Sci. **24** (7), 857–866 (1993).

Translated by O. Bazhenov